Largely Color-Tuning Prompt and Delayed Fluorescence: Dinuclear Cu(I) Halide Complexes with *tert*-Amines and Phosphines

Ke Xu[a], Bu-Lin Chen[a], Fei Yang[b], Li Liu*[a], Xin-Xin Zhong*[a], Lei Wang*[b], Xun-Jin Zhu[c], Fa-Bao Li[a], Wai-Yeung Wong*[d], Hai-Mei Qin[e]

[a] *Ministry of Education Key Laboratory for the Synthesis and Application of Organic Functional Molecules, Hubei University, Wuhan 430062, P. R. China.*
[b] *Wuhan National Laboratory for Optoelectronics, Huazhong University of Science and Technology, Wuhan 430074, P. R. China.*
[c] *Department of Chemistry, Hong Kong Baptist University, Hong Kong, P. R. China*
[d] *Department of Applied Biology and Chemical Technology, The Hong Kong Polytechnic University, Hong Kong, P. R. China.*
[e] *Department of Chemistry, Xiamen University, Xiamen 361005, P. R. China.*

ABSTRACT

Luminescent copper(I) halide complexes with bi- and tri-dentate rigid ligands have gained wide research interests. In this paper, six tetracoordinate dinuclear copper(I) halide complexes $Cu_2X_2(ppda)_2$ [ppda = 2-[2-(dimethylamino)phenyl(phenyl)phosphino]-N,N-dimethylaniline, X = I (**1**), Br (**2**), Cl (**3**)] and $Cu_2X_2(pfda)_2$ [pfda = 2-[2-(dimethylamino)-4-(trifluoromethyl)phenyl(phenyl)phosphino]-N,N-dimethyl-5-trifluoro methylaniline, X = I (**4**), Br (**5**), Cl (**6**)], were successfully prepared and systematically characterized on their structures and photophysical properties. Complexes **1-5** have a centrosymmetric form with a planar Cu_2X_2 unit, complex **6** has a mirror symmetry form with a butterfly-shaped Cu_2X_2. Solid complexes **1**, **4** and **5** emit delayed fluorescence at room temperature, intense blue to greenish yellow (λ_{max} = 443–570 nm) light and their peak wavelengths are located at 443–570 nm with microsecond lifetimes (τ = 0.4–19.2 μs, Φ_{PL} =

0.05–0.48), while complexes **2**, **3** and **6** show prompt fluorescence, very weak yellowish green to yellow (λ_{max} = 534–595 nm) emission with peak wavelengths at 534–595 nm and lifetimes in nanoseconds (τ = 4.4 –9.3 ns, Φ_{PL} < 0.0001). (Metal+halide) to ligand and intraligand charge transitions are main origin of the emission of the complexes. Solution-processed, complex **3**-based nondoped and doped devices emit yellow and yellow green light with CIE coordinated at (0.48, 0.48) and (0.41, 0.51), respectively. Doped device achieved a maximum EQE up to 3.12%, and luminance of 2280 cd/m^2.

1. INTRODUCTION

Copper(I) complexes are regarded as potential options for a realistic way to construct low cost and high efficiency OLEDs due to their rich structural and luminescent properties.[1-9] These complexes usually have small $\Delta E(S_1\text{-}T_1)$ values caused by small overlapped HOMO and LUMO orbitals, from which efficient room-temperature TADF can benefit. Therefore, the emission of copper(I) complexes can combine singlet with triplet excitons by efficient reverse intersystem crossing.[10-14]

Previous studies reveal that three-coordinate planar Cu(I) complexes coordinated with rigid ligands[15] or two-coordinate linear Cu(I) complexes[16] can suppress the geometric distortion of Cu(I) center by excitation. Osawa's group reported green OLEDs containing three-coordinate mononuclear Cu(I) halide complexes chelating rigid diphosphine ligand with EQE over 20%.[15] A recent paper by Thompson *et al*. has reported blue emitting two-coordinate Cu(I) complexes based OLEDs with a EQE of 9.0%.[16] Bulky or bridged ligands are used to construct a firm framework to decrease nonradiative decay as well.

Recently, a tridentate phosphine ligand was adopted by Xu's group to synthesize a tetracoordinate mononuclear Cu(I) iodide complex in highly rigid coordination geometry, which showed a EQE up to 16.3%.[17]

Dinuclear Cu(I) cores possess a great advantage over mononuclear core since they have rigid structure and thus high efficiency recorded for bulky ligand chelated complexes[18-24]. However, the reported dinuclear Cu(I) halide complexes are mainly limited to bidendate diphoshines[20,24-31] or imine and phosphine[18,21-23,32-36] ligands, whereas bidentate amine and phosphine ligands are rarely reported. In comparison to the great success in green emitters, it seems that blue emitters are still a challenge to meet with the requirement of full color displays and white light sources.[37,38]

With great interests to explore highly efficient blue emitters[39-42] and study the relationship of structure-property of complexes, two electron-donating NMe_2 groups are combined into the *ortho*-position of two P-linked phenyl rings in ligand **ppda**, two electron-withdrawing CF_3 groups are introduced into the *meta*-position of NEt_2 in ligand **pfda** to change the emissive color. Complexes **1-5** have planar Cu_2X_2 core, while complex **6** has a butterfly-shaped Cu_2X_2 core. They showed very different emissions from previously reported ones. Here, the structures, photophysical and redox properties together with theoretical calculations of complexes **1-6** are reported. Also the OLED devices based on complex **4** were fabricated via solution-processed method and their electroluminescent behaviors are studied.

2. EXPERIMENTAL SECTION

2.1. Synthesis of pfda. At −78°C, *n*-BuLi (2.5 M in hexane, 2.4 mL, 6 mmol) was added

dropwise to a THF (10 mL) solution of 2-bromo-N,N-dimethyl-5-(trifluoromethyl)aniline (1.6 g, 6 mmol) , and stirred for 30 min. Later $PhPCl_2$ (0.39 mL, 3 mmol) was added in 5 min, and the subsequent reaction mixture was allowed to slowly warm to room temperature. After being stirred overnight, the reaction was quenched by the addition of water (10 mL) and then treated with aqueous NH_4Cl, CH_2Cl_2 (3 × 10 mL) was used to extract the mixture and the combined extracts were dried by anhydrous Na_2SO_4, filtered, and concentrated to give a residue. The residue was further purified by chromatography, and obtained a white powder of 0.68 g (47% yield).

2.2. Synthesis of complexes 1-6. All Cu(I) complexes were prepared by the following method. A mixture of copper(I) halide (1 mmol) and **ppda** or **pfda** (1 mmol) in 30 mL of CH_3CN was stirred for 2 days at room temperature to form a suspension which was then filtered off. The filtrate was concentrated to give a residue. The residue was dissolved in CH_2Cl_2/CH_3CN, and complexes were obtained as colorless crystals for **1**, and yellow crystals for **2-6** after slow evaporation at room temperature.

3. RESULTS AND DISCUSSION

3.1. Syntheses and Characterizations. Scheme 1 presents the synthetic routes to **ppda**, **pfda**, and complexes **1-6**. The synthesis of 2-dimethylamino-5-(trifluoromethyl)phenyllithium was accomplished in a mixture of 2-bromo-N,N-dimethyl-5-(trifluoromethyl)aniline and *n*-butyllithium with the equal mole in THF at −78°C under nitrogen. After the addition of $PPhCl_2$ to 2-dimethylamino-5-(trifluoromethyl)phenyllithium, **pfda** was prepared in 47% yield. Complexes **1-6** were obtained in 76−84% yields by the reaction of CuX in acetonitrile

with 1 equivalent of **ppda** and **pfda**, respectively. Six complexes are stable in air and dissolved in solvents of acetonitrile and chloroform. Their structures were identified (Figures 1, S1-S22).

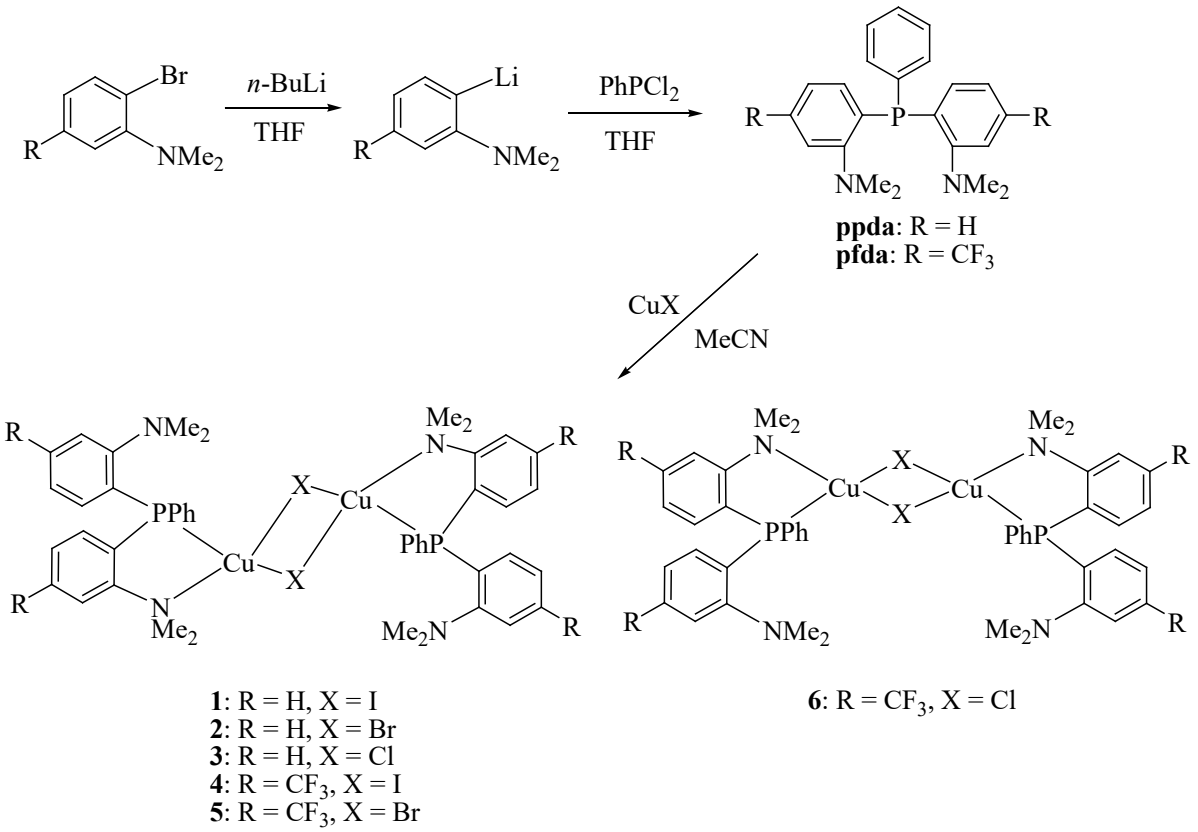

Scheme 1. Synthetic pathways to ligands **ppda**, **pfda** and complexes **1-6**.

Table 1. Some bond lengths [Å] and angles (°) of complexes 1-6

Complex	**1**	**2**	**3**	**4**	**5**	**6** • CH_3CN
Cu2–X1	2.5823(5)	2.4506(3)	2.3255(5)	2.6937(6)	2.5927(4)	2.3329(9)
Cu1–X1	2.7547(5)	2.4721(4)	2.3240(5)	2.5425(6)	2.3713(4)	2.3364(9)
Cu1–X2	2.5823(5)	2.4506(3)	2.3255(5)	2.6937(6)	2.5927(4)	2.3260(10)
Cu2–X2	2.7547(5)	2.4721(4)	2.3240(5),	2.5425(6)	2.3713(4)	2.3263(9)
Cu1–P1	2.2574(8)	2.2012(5)	2.1782(4)	2.2355(8)	2.2025(6)	2.1922(9)
Cu2–P2	2.2574(8)	2.2012(5)	2.1782(4)	2.2355(8)	2.2025(6)	2.1875(9)
Cu1–N1	2.292(3)	2.2899(13)	2.3692(16)	2.352(2)	2.3495(19)	2.354(3)
Cu2–N2	2.292(3)	2.2899(13)	2.3692(16)	2.352(2)	2.3495(19)	2.345(3)
Cu1⋯Cu2	3.471	3.133	3.072	3.053	3.050	3.014

P1–Cu1–N1	82.64(7)	84.54(3)	82.41(4)	81.06(5)	81.58(5)	82.88(7)
P2–Cu2–N2	82.64(7)	84.54(3)	82.41(4)	81.06(5)	81.58(5)	83.33(7)
X1–Cu1–X2	98.937(16)	100.956(10)	97.278(16)	108.74(2)	104.336(13)	97.50(3)
X1–Cu2–X2	98.937(16)	100.956(10)	97.278(16)	108.74(2)	104.336(13)	97.61(3)
Cu1–X1–Cu2	81.062(16)	79.043(10)	82.722(16)	71.26(2)	75.664(13)	80.39(3)
Cu1–X2–Cu2	81.062(16)	79.043(10)	82.722(16)	71.26(2)	75.664(13)	80.75(3)
X1-Cu2-Cu1-X2	0	0	0	0	0	160.82

Table 2. **The dihedral angles between the CuX_2 plane and bridging N,P phenyl ring in complexes 1-6**

Complex	Dihedral angle (°)	Complex	Dihedral angle (°)
1	67.31	**4**	70.81
2	85.52	**5**	70.23
3	88.18	**6**	82.53

Figure 1 presents the perspective views of complexes **1-6** and Tables S1 and 1 give the crystallographic data and some bond lengths and angles. One solvent CH_3CN molecule is in complex **6**. Two copper(I) are in tetrahedrally connected with two halogen atoms and a N and a P from the **ppda** and **pfda** ligands, respectively. Complexes **1-5** have a planar Cu_2X_2 with centrosymmetry, while complex **6** has a mirror symmetric form with a butterfly-shaped Cu_2X_2 where Cu and Cl atoms are not located in one plane with distinct dihedral angle Cl1-Cu2-Cu1-Cl2 of 160.82°. We found that, as the X radius increases, the bond lengths of Cu–X increase (Table 1). This trend is also found in the Cu1⋯Cu2 distances, which were widely reported to have important impacts on the emission of the multinuclear Cu(I) halide complexes. The Cu1⋯Cu2 distances are in the range of 3.014 and 3.471 Å (the sum of van der Waals radius of copper is 2.8 Å), indicating negligible interaction between two Cu atoms in complexes **1-6**. Careful contrast of previously reported $Cu_2X_2(PNMe_2)_2$ ($PNMe_2$ =

Ph_2P-(*o*-C_6H_4)-NMe_2) having nonplanar mirror symmetry and a butterfly-shaped Cu_2X_2 core (X = I and Br),[19] the introduction of two NMe_2 into the ligand **ppda** in complexes **2** and **3**, leads to a structural change. A planar centrosymmetry motif and a larger Cu1···Cu2 distance is ascribed to the increased sterical requirement of **ppda**. The structures of central Cu_2X_2 unit of complex **3** and $Cu_2Cl_2(PNMe_2)_2$ are similar, both of which are planar centrosymmetry, and have similar Cu1···Cu2 distance (3.072 Å for **3** and 2.983 Å for $Cu_2Cl_2(PNMe_2)_2$). When two CF_3 groups are introduced into the ligand **pfda**, complexes **4** and **5** still have a centrosymmetric form with a planar Cu_2X_2 except complex **6**, and the Cu1···Cu2 distances in complexes **4-6** are shortened. The dihedral angles between the CuX_2 plane and bridging N,P phenyl ring plane in complexes **1-6**, are shown in Table 2 and Figures S23–S28. The dihedral angles are in the order of **1** < **5** < **4** < **6** < **2** < **3**. The two planes in complexes **2**, **3** and **6** are close to orthogonal.

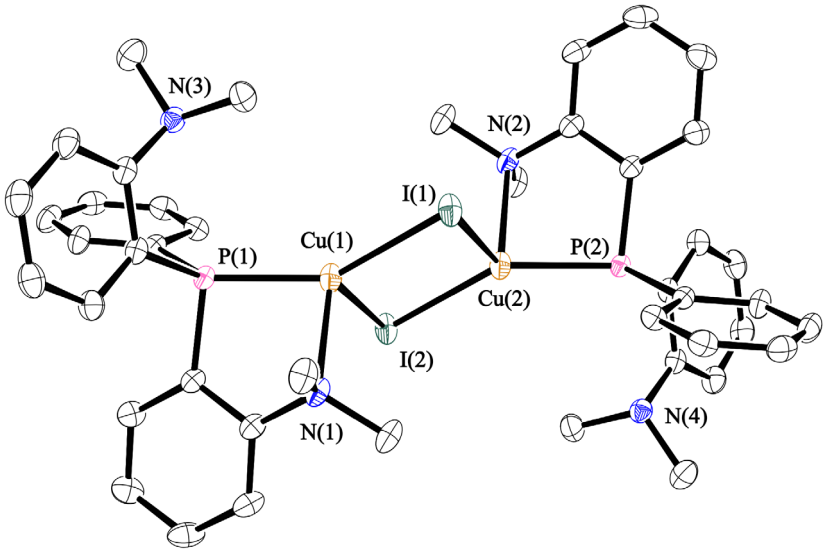

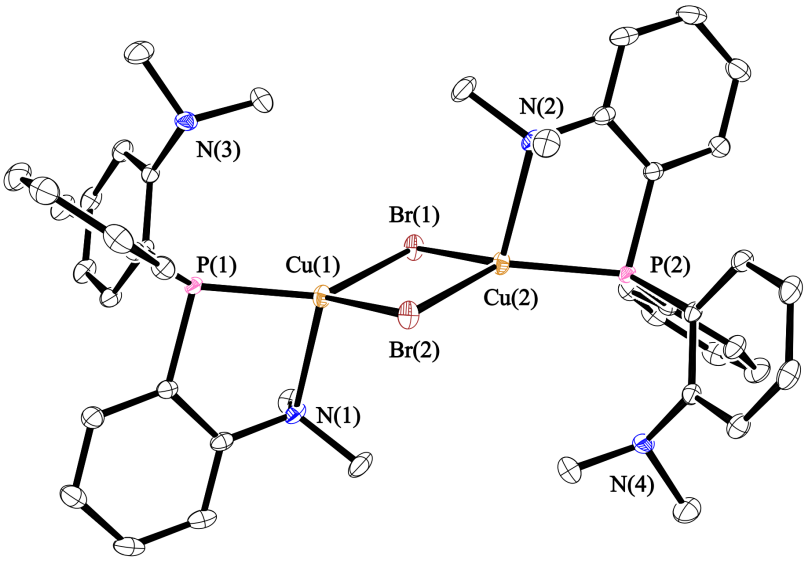

2

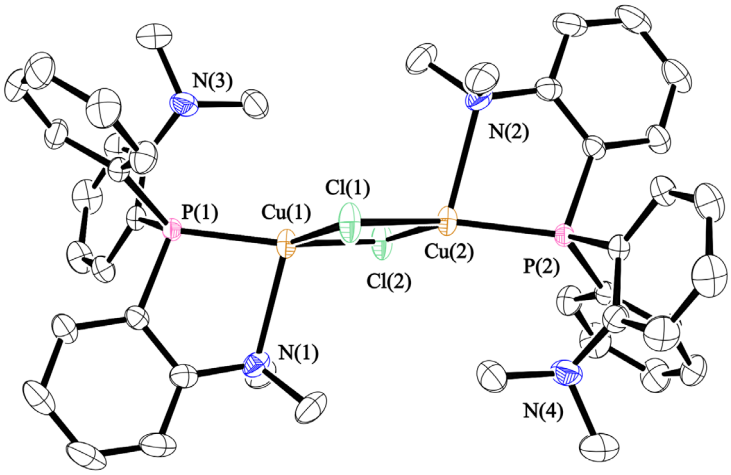

3

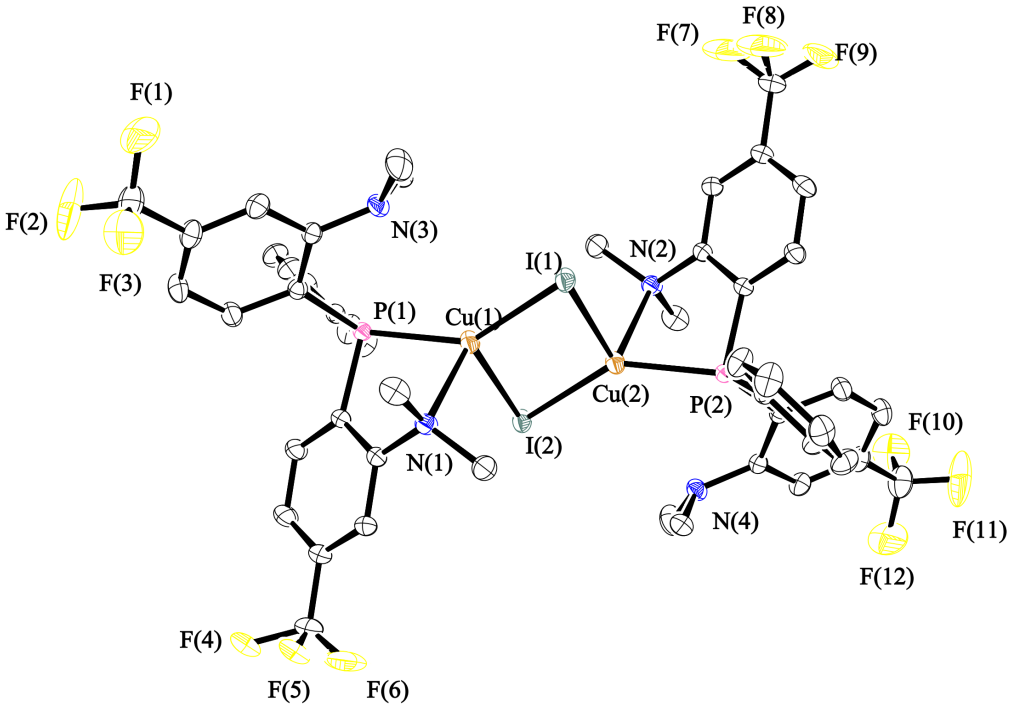
F(8)
F(7)
F(9)
F(1)
F(2)
F(3)
N(3)
I(1)
N(2)
P(1)
Cu(1)
Cu(2)
P(2)
F(10)
I(2)
N(1)
N(4)
F(11)
F(12)
F(4)
F(5)
F(6)

4

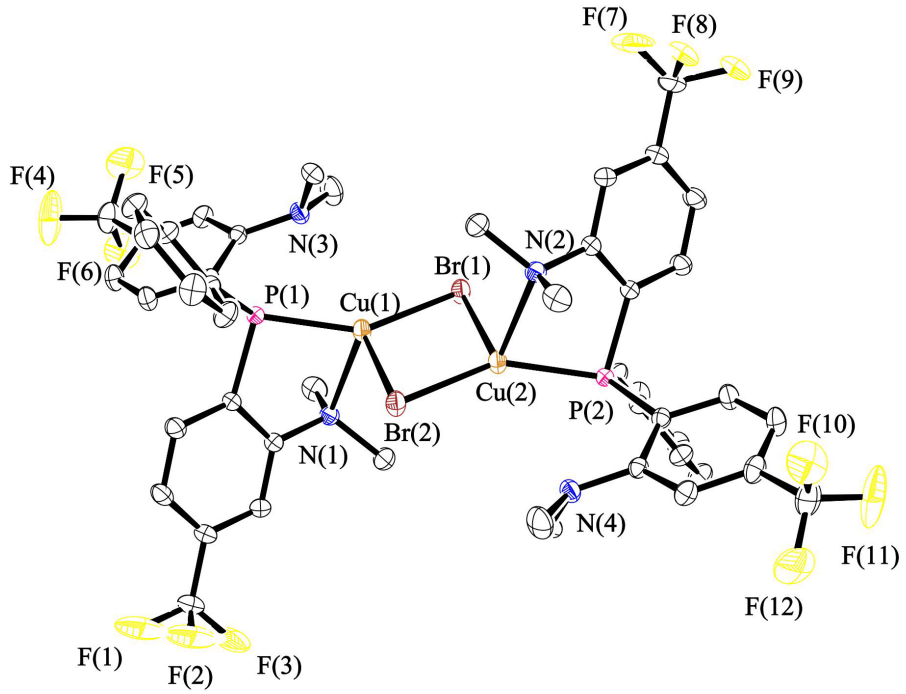
F(7)
F(8)
F(9)
F(4)
F(5)
N(3)
N(2)
F(6)
Br(1)
P(1)
Cu(1)
Cu(2)
P(2)
F(10)
Br(2)
N(1)
N(4)
F(11)
F(12)
F(1)
F(2)
F(3)

5

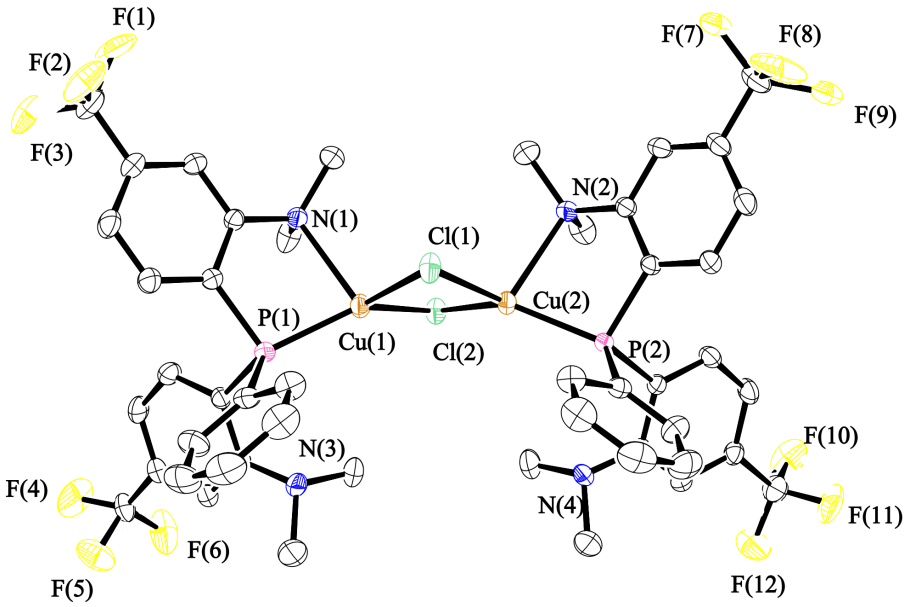

6

Figure 1. ORTEP diagrams of **1-6**.

3.2. Photophysical, Redox Properties and Theoretical Calculations. The absorption spectra of ligands **ppda**, **pfda** and complexes **1-6** in CH_2Cl_2 (4×10^{-5} M) at room temperature are displayed in Figure 2. The absorption spectra exhibit bands at 259 and 300 nm for **ppda**, 266 and 318 nm for **pfda**, which are ascribed to n→π* and π→π* transitions of arylphosphine and arylamine. The absorption peak wavelength of **pfda** is red-shifted about 7 ~ 18 nm than **ppda**. Complexes **1-3** show absorption peaks (269–271 nm), shoulders (305–314 nm) and tails (350–415 nm), and red-shifted bands are found in complexes **4-6** (274–278, 331–340, and 375–435 nm, respectively). TDDFT calculations (Figures 3, S44–S50, Tables S3–S8) show that the transitions from HOMO to LUMO contribute to the lowest excited states for complexes **1** and **4-6**, whereas for complexes **2** and **3**, the transitions are from HOMO to LUMO+1. The shapes of HOMO show that the electrons in HOMO are largely concentrated

on the Cu, X, P and N atoms, while the LUMO levels primarily distribute to the bridging N,P phenyl rings in ligands, similar cases are found in LUMO+1. Therefore the lowest excited states are composed of (metal+halide)-to-ligand and intraligand charge transitions. Similar red-shifting (5 ~ 26 nm) are observed for the absorption bands of **4-6** when compared with **1-3**, which is attributed to the reduced LUMO level by electron-withdrawing CF_3.

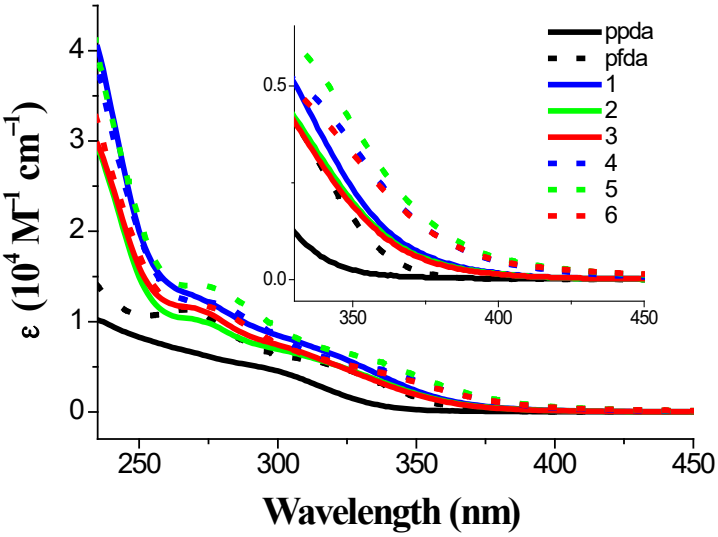

Figure 2. Absorption spectra of **ppda**, **pfda** and complexes **1-6** in CH_2Cl_2 at r.t. The Inset is a magnified absorption edges.

complex	The optimized S_0 geometry	HOMO (eV)	LUMO (eV)
1	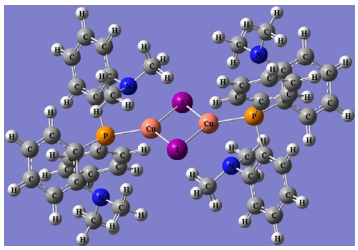	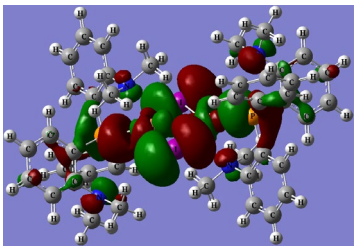 –5.25	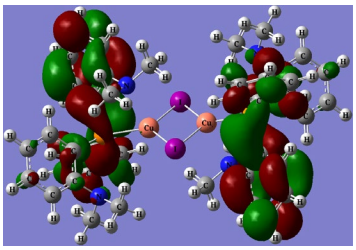 –1.17
2	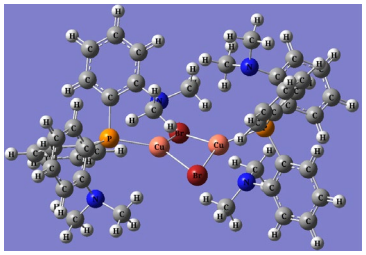	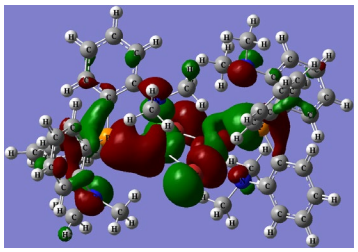 –5.32	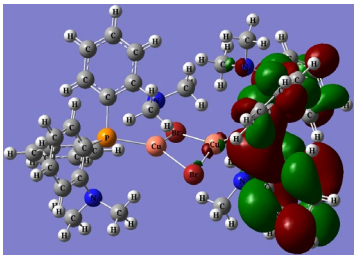 –1.19

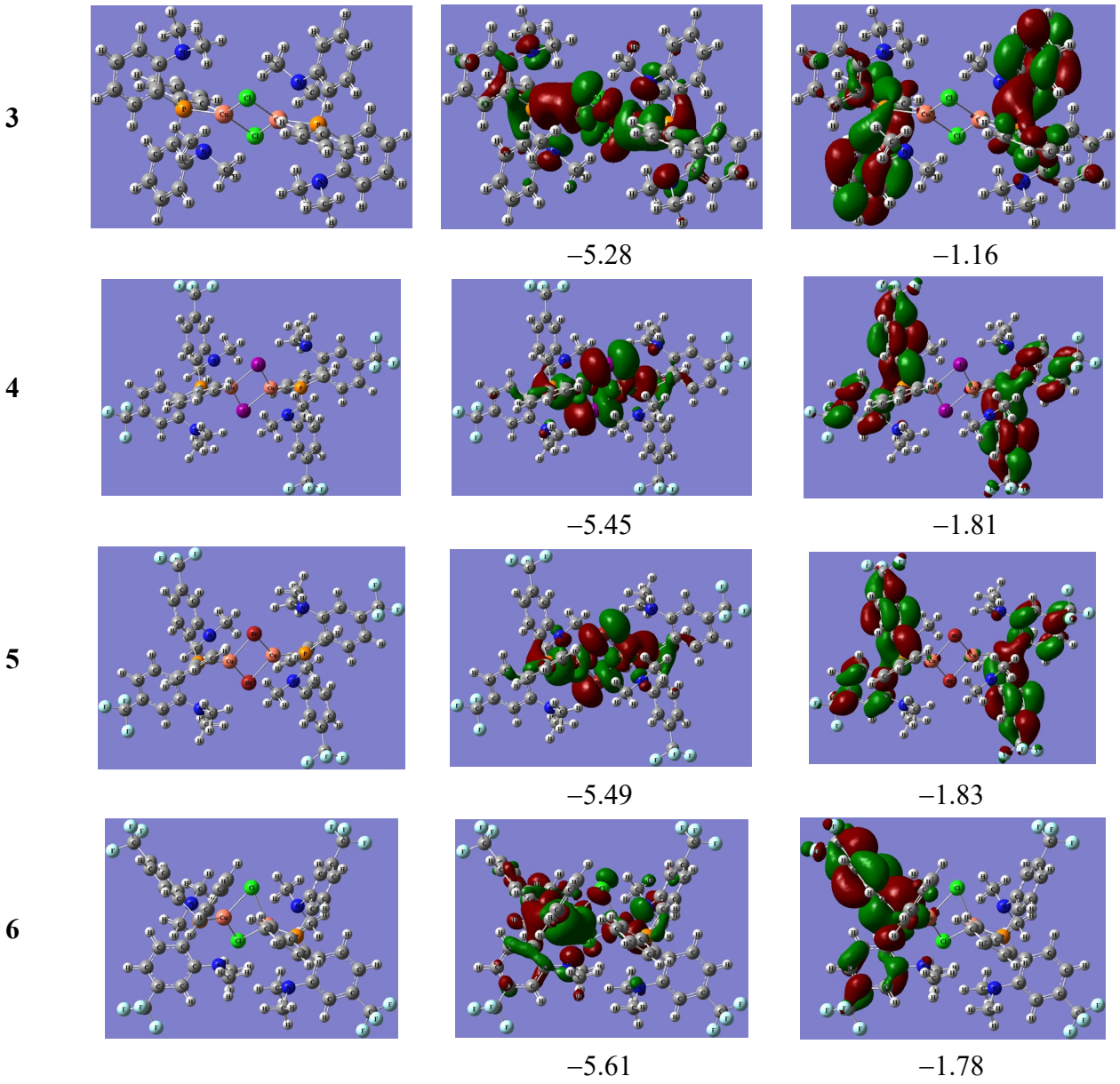

Figure 3. The S_0 geometry optimized, shapes of HOMO and LUMO of **1-6**.

The electrochemical properties of **1-6** were determined by cyclic voltammetry (CV). Cyclic voltammogram of complexes **1-6** in 10^{-3} M CH_2Cl_2 and $TBAPF_6$ (0.1 M), potential data, energy levels and gaps are shown in Figure S29 and Table S9. Cathodic peak potentials of complexes **1-6** are located at ca. –0.94 ~ –1.70 V, which correspond to the reduction of ligand. The first and second anodic waves were attributed to the oxidation of Cu^+ and ligand, respectively. Compared with the lowest potential of complex **3**, complex **1** has the highest

first anodic wave indicating a good stabilization of Cu^{+}. We speculate that the electronic effect of groups linked to Cu^{+} center is not the main reason but steric hinderance which suppresses the distortion of geometry from tetrahedron to square planar, so the oxidation of Cu^{+} becomes more difficult and the resulting Cu^{2+} is therefore more destabilized.

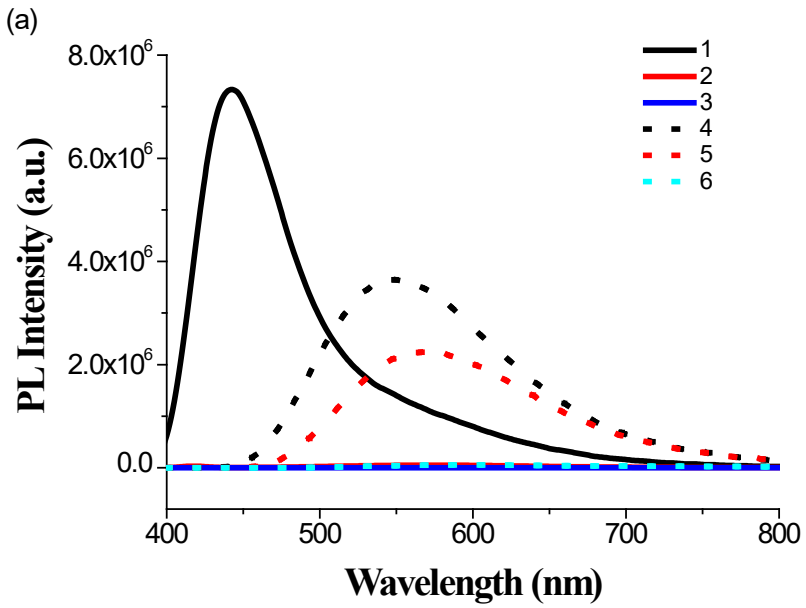

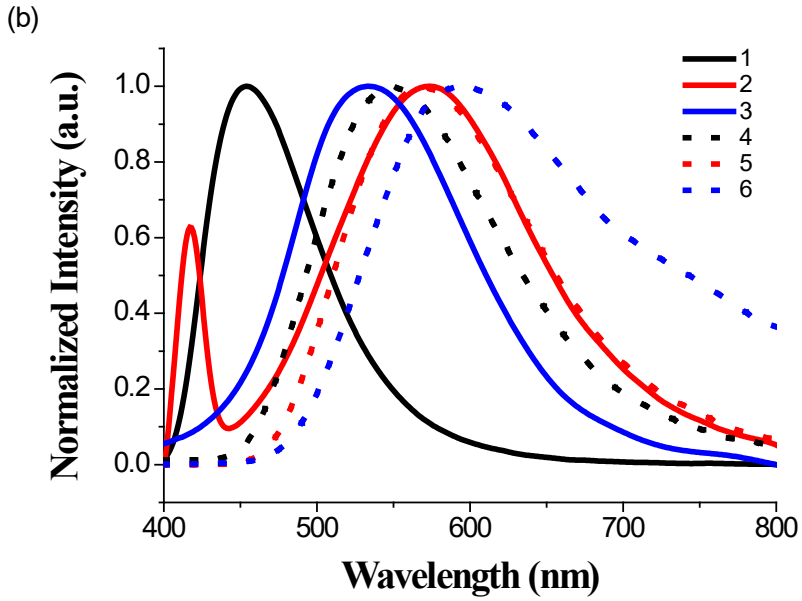

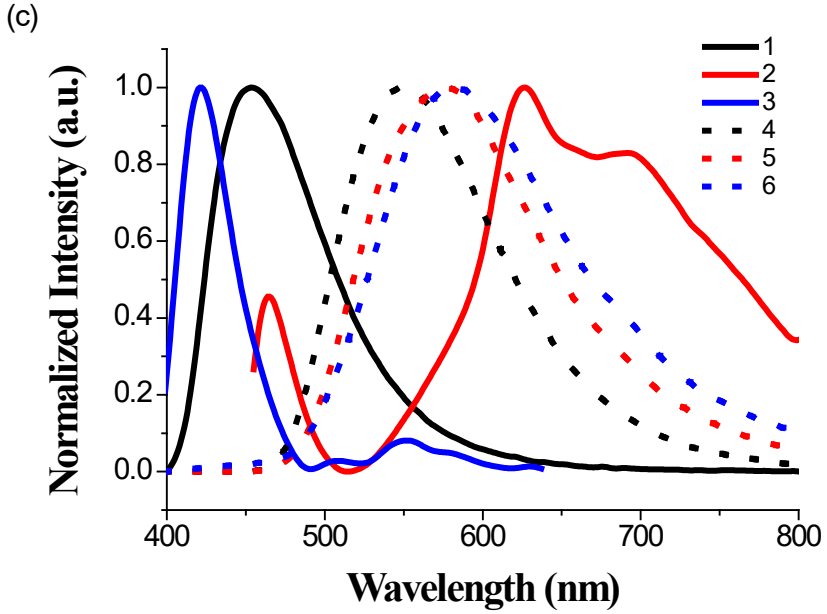

Figure 4. Emission and normalized emission spectra of **1-6** in solid at 297 K (a, b, λ_{ex} = 365 for **1**, 375 for **2** and **3**, 378 nm for **4-6**) and 77 K (c, λ_{ex} = 365 for **1**, 420 for **2**, 360 for **3** and **5**, 378 nm for **4** and **6**).

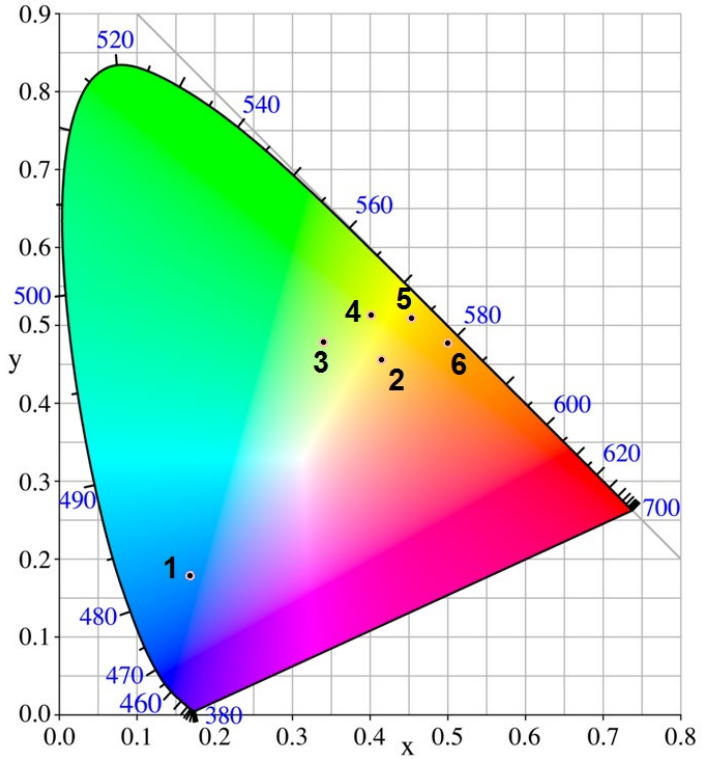

Figure 5. CIE graph of complexes **1-6**.

Table 3. **Photophysical data of 1-6 in solid**

	λ_{max} (nm)[a]		τ (μs)[b]		Φ[c]	k_r[d] ($10^5 s^{-1}$)	$E(S_1)$[e] (eV)	$E(T_1)$[e] (eV)	ΔE (S_1-T_1)[e] (eV)	λ (nm)[f]
	297 K	77 K	297 K	77 K	297 K	297 K				
1	443	454	19.2	577	0.48	0.25	3.2461	3.1392	0.1069	/
2	417*, 574	465*, 626	0.0057	2.1	< 0.0001	/	2.8182	2.4125	0.4047	549
3	534	422, 552*	0.0093	0.00048	< 0.0001	/	2.9594	2.5410	0.4184	584
4	548	551	1.1	112	0.11	1.00	2.9040	2.7373	0.1667 0.1085[g]	611
5	570	576	0.4	202	0.05	1.25	2.8506	2.7556	0.095	617
6	595	582	0.0044	1.7	< 0.0001	/	2.9314	2.5941	0.3373	520

[a] Emission peak wavelength. Asterisks indicate that emission peaks appear as shoulders or weak bands. [b] Average lifetime. [c] Absolute emission quantum. [d] Radiative decay rate constant. $k_r = \Phi/\tau_{ave}$. [e] The S_1 and T_1 energy levels were estimated based on the emission peak onsets at 297 K and 77 K. [f] Calculated emission wavelengths according to the S_1 geometries optimized. [g] $E(S_1)$ and $E(T_1)$ are the vertical excitation energies, $\Delta E(S_1–T_1) = E(S_1) – E(T_1)$.

Complexes **1, 4** and **5** show intense blue to greenish yellow emissions (443–570 nm) with Φ_{PL} = 0.05–0.48, complexes **2, 3** and **6** exhibit very weak greenish yellow to yellow emissions (534–595 nm) with Φ_{PL} < 0.0001 at 297 K (Figure 4, Table 3). The emission maxima of **1** is blue-shifted by 31 nm than previously reported $Cu_2I_2(PNMe_2)_2$,[19] as we anticipated, two electron-donating NMe_2 on the *ortho*-position of P-linked phenyl rings in ligand **ppda** can raise LUMO level. To the best of our knowledge, this has been so far the firstly reported efficient blue light with emission maxima shorter than 440 nm from neutral dinuclear Cu(I) halide complexes. Based on the emission curve in solid at 297 K, the CIE color coordinates of complexes **1-6** are (0.168, 0.179), (0.415, 0.456), (0.339, 0.478), (0.401, 0.514), (0.453, 0.510) and (0.500, 0.478), respectively (Figure 5). Large red-shifting of 61 ~ 105 nm for the emission bands of complexes **4** and **6** are found in comparison to **1** and **3**,

possibly ascribed to two electron-withdrawing CF_3 which lower the LUMO level. The emission maxima of **5** is blue-shifted by 4 nm than **2**. According to the TDDFT calculation, the emission properties of complexes **2-6** were also estimated (the optimized S_1 geometry of complex **1** was failed even if tried many methods). The calculated emission wavelengths of complexes **2-5** (Table 3) are in accord with the experimental data. The contribution to the emission of complexes **2-6** are mainly come from LUMO→HOMO transition. The shapes of HOMOs and LUMOs and S_1 state geometries are presented in Figure 6. The HOMOs are mostly confined to Cu, X, and P and N in ligands **ppda** and **pfda**, and the LUMOs are largely concentrated on the bridging N,P phenyl ring. Therefore the emission primarily comes from (metal+halide) to ligand and intraligand charge transitions.

complex	The optimized S_1 geometry	HOMO (eV)	LUMO (eV)
2	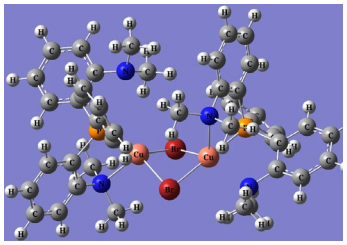	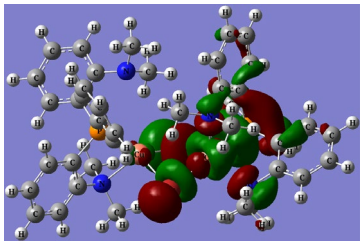	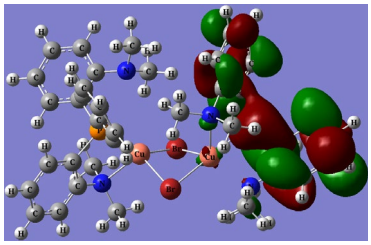
		–3.95	–1.74
3	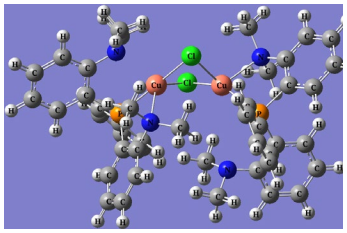	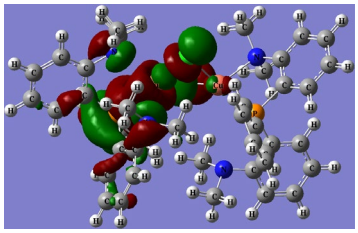	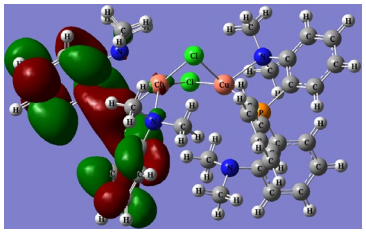
		–3.92	–1.69

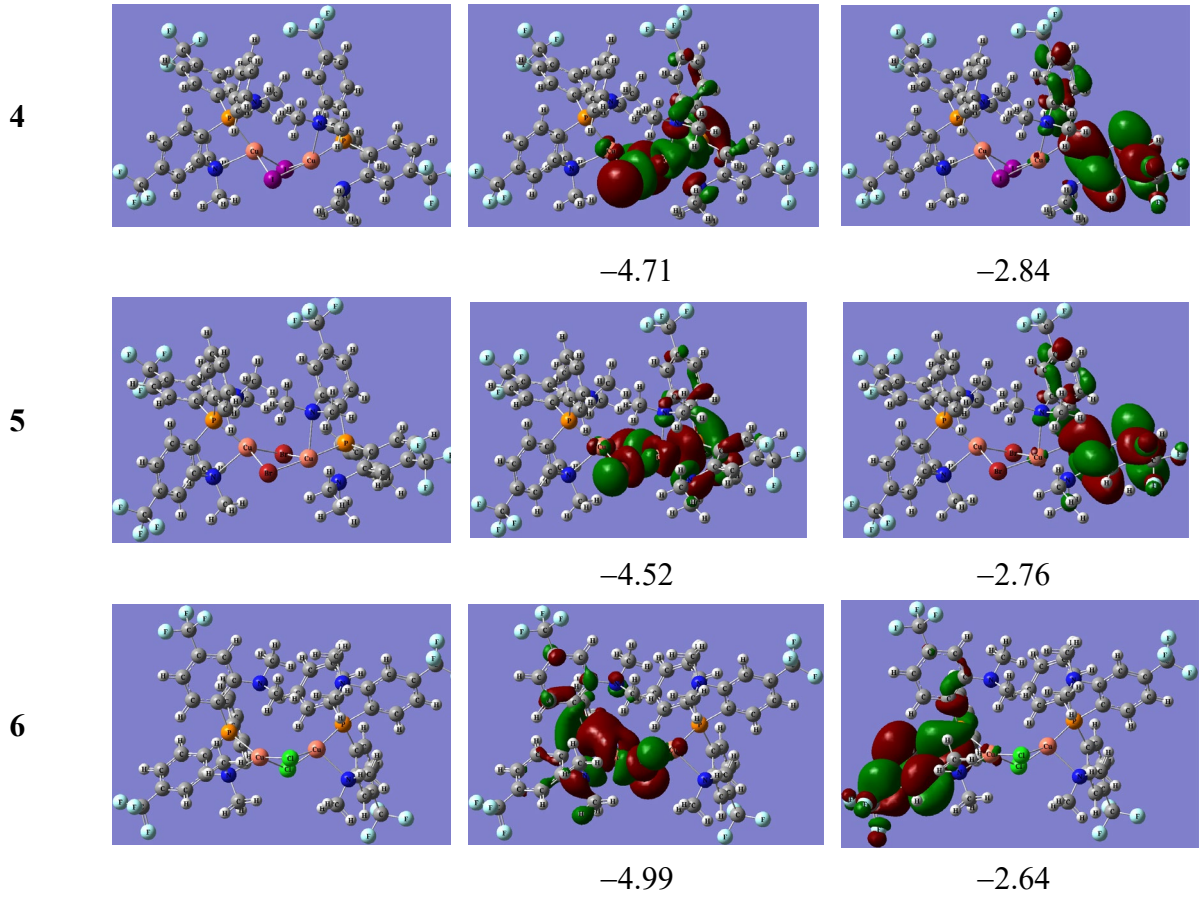

Figure 6. The S_1 geometry optimized and shapes of HOMO and LUMO of **2-6**.

The emission peak wavelengths of complex **1-6** are located at 422–626 nm at 77 K. The emission curves of **1**, **2**, **4** and **5** are red-shifted than that at 297 K, and can be explained by the dominated the thermal population of a lower excited state (T_1) at low temperature.[42] While for complexes **3** and **6**, blue-shifting of the emission bands can be attributed to the changes of vibrations and rotations that suppressed the energy relaxation of excited state.[42] The lifetimes (Table 3, Figures S32-S43) of **1**, **4**, and **5** at 297 K are 19.2, 1.1 and 0.4 μs, respectively, which are 30 ~ 505 times shorter than that at 77 K, exhibiting possible exist of different emission inter-exchangeable and thermally activated process.[19] Based on the fluorescence and phosphorescence spectra onsets, the S_1 and T_1 energy levels are estimated (Table 3, Figure 4),

and $\Delta E(S_1-T_1)$ values are at 0.095–0.1667 eV for complexes **1**, **4** and **5**, indicating they show efficient thermally activated delayed fluorescence.[13-14,19] While complexes **2**, **3** and **6** do not show efficient TADF behaviors, which are ascribed to the much larger $\Delta E(S_1-T_1)$ values (0.3373 ~ 0.4184 eV), that is why they display prompt fluorescence with nanosecond lifetimes (4.4 ~ 9.3 ns). Additionally, the dihedral angles between CuX_2 plane and bridging N,P phenyl ring plane, are much larger in complexes **2**, **3** and **6** (82.53 ~ 88.18°) than in complexes **1**, **4** and **5** (67.31 ~ 70.81°) (Table 2 and Figures S23–S28). Generally, $\Delta E(S_1-T_1)$ relies on the exchange integral between S_1 and T_1, or approximated between HOMO and LUMO.[43] The less overlap between the frontier orbitals, the less mixing of these states, thus the less $\Delta E(S_1-T_1)$ value, which also results in less distortion upon excitation and helps to increase the PLQY.[44-47] So, substituted groups can play very important role to sterically control the orientation of ligands and vary photophysical property of complexes. The radiative rate constant k_r of complexes **1**, **4** and **5** were calculated to be 2.5×10^4 to 1.25×10^5 s^{-1}, similar with previously reported Cu(I) halide complexes $Cu_2X_2(PNMe_2)$.[19]

To confirm the existence of TADF, complex **4** was as a representative and measured its decay times (τ_{obs}) in the temperature range between 77 K and 297 K (Figure 7). Thermally equilibrated S_1 and T_1 states assumed, the relationship between the decay time and temperature is shown in eq(1):

$$\tau_{obs} = \frac{1 + \frac{1}{3}\exp\left(-\frac{\triangle E_{ST}}{K_B T}\right)}{\frac{1}{\tau(T_1)} + \frac{1}{3\tau(S_1)}\exp\left(-\frac{\triangle E_{ST}}{K_B T}\right)} \quad (1)$$

where K_B, T, $\tau(S_1)$, $\tau(T_1)$ and ΔE_{ST} are the Boltzmann constant, the absolute temperature, the lifetimes of S_1, T_1, and the energy separation between S_1 and T_1, respectively. In the temperature range, the lifetime is single-exponential. Eqn (1) is fitted to the lifetime measured at various temperatures, then lifetimes at S_1 (10.32 ns) and T_1 (108.7 μs), and ΔE_{ST} (0.103 eV) were obtained. The short lifetime of 10.32 ns substantiates its S_1 character. Therefore, the lifetime at 297 K of τ = 1.1 μs stands for a delayed fluorescence. The fitted (T_1) lifetime (108.7 μs) approximates to the measured lifetime of 112 μs of **4** at 77 K, and the ΔE_{ST} (0.103 eV) is similar to the calculated one (0.1085 eV) (Figure 7, Table 3). At temperatures below 100 K, complex **4** emits almost pure phosphorescence. As the temperature increases, the emission from the phosphorescence (T_1) decreases, and accordingly, the emission from the TADF increases.

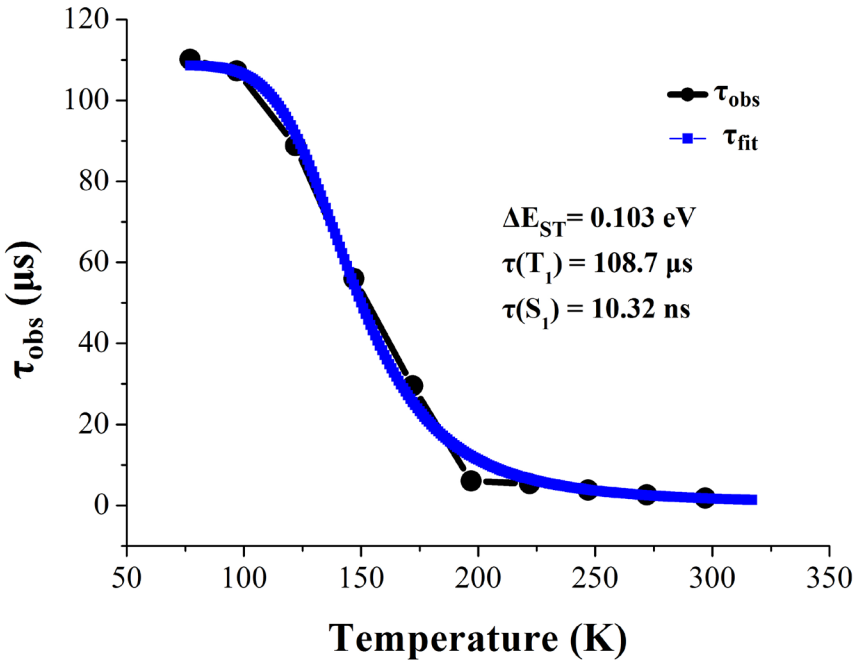

Figure 7. Temperature versus decay lifetime of complex **4** and a fit curve.

By TDDFT calculation, the coordinative geometris of Cu center in the optimized S_0, S_1

and T_1 (Table S1 and Figure S51), are tetrahedrally distorted. P–Cu–N bond angles in S_0 and S_1 geomerties nearly remain unchanged. This can be attributed to the rigid ligands **ppda** and **pfda**. Larger changes in bond angles of P–Cu–X, N–Cu–X and X–Cu–X, may lead to Jahn-Teller distortion of excited states[15] and thus lower emissive intensity.

3.3. Thermal properties. For OLED applications, good thermal stabilities of emissive materials are required. Thus thermogravimetric analysis (TGA) under nitrogen for complexes **1-6** was conducted to determine the onset decomposition temperatures (T_{dec}). It was found that **1-6** are thermally stable, with the T_{dec} values over 250 °C (Figure 8, 305-367 °C for the complexes **1-3**, and 268-281 °C for the complexes **4-6**), which meets the demand for OLED operating temperature. The introduction of two CF_3 groups in ligand **pfda** can make complexes **4-6** decompose more easily, ascribed to the distinct elongation of Cu–N and Cu–P bonds in complexes **4-6**. Complex **1-3** lose ca. 61-77% weight at 419 ~ 486 °C, and complexes **4-6** lose ca. 69~85% weight at 307 ~ 354 °C, which corresponds to the loss of two ligands **ppda** and **pfpa**.

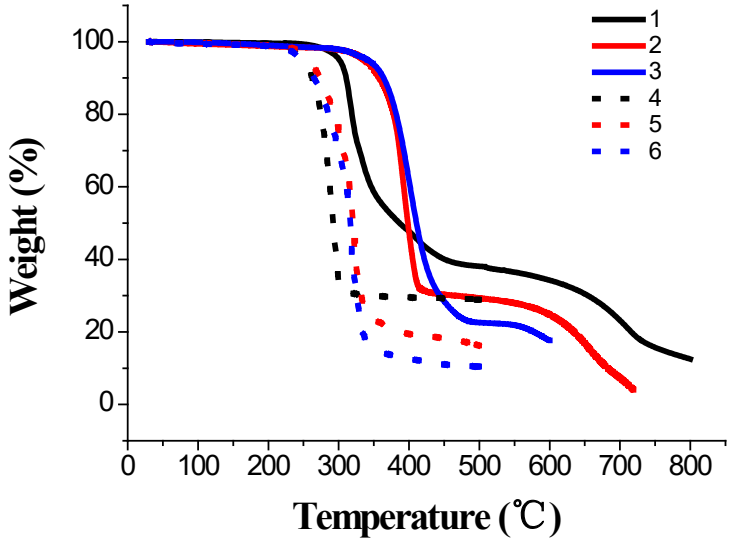

Figure 8. TGA curves of complexes **1-6**.

3.4. Electroluminescent properties. Complex **4** was used as the emitting material in solution-processed devices with the structure of ITO/PEDOT:PSS (40 nm)/complex **4** (20 nm)/TPBi (30 nm)/LiF (1 nm)/Al (100 nm). (ITO: anode; Al: cathode; PEDOT: PSS: hole injection layer, TPBi: electron transporting layer; LiF: electron injecting layer). Figure 9(a) shows the energy level diagram. This device emits yellow green light (λ_{em} = 564 nm) with CIE coordinated at (0.41, 0.51). Figure 9(c) and Figure 9(d) present the EQE up to 0.17% and the maximum luminance reaches 75.52 cd/m^2. Additionally, several doped devices with CBP as host materials were fabricated. But the doped devices did not exhibit satisfactory results (Figure S52), which is possibly ascribed to the mismatching of CBP and complex **4** in energy level. Therefore, a matching host material is required to enhance device performance.

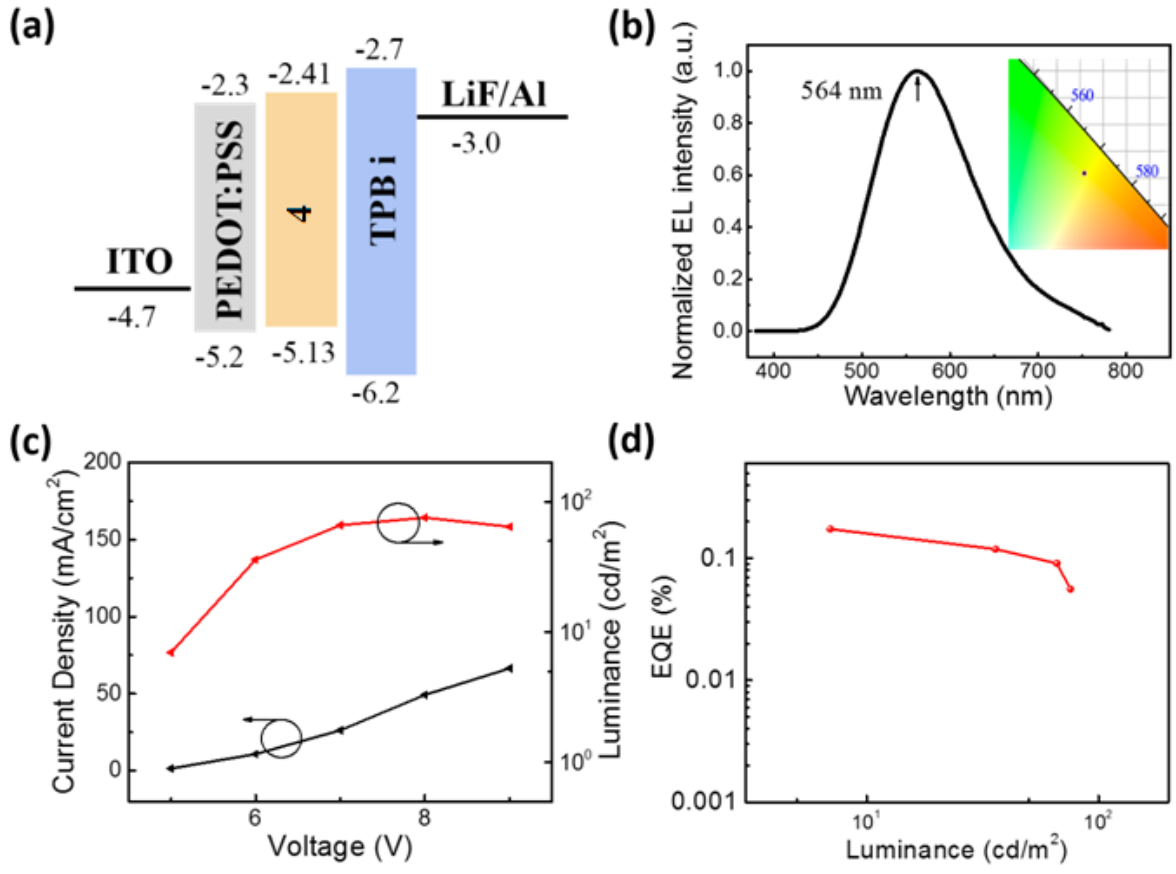

Figure 9. (a) Energy-level drawing of the device; (b) Electroluminescence spectra and

corresponding CIE; (c) J–V–L characteristics; (d) EQE–luminance characteristics.

4. CONCLUSIONS

It is the firstly reported efficient blue light with emission maxima shorter than 440 nm from dinuclear Cu(I) halide complexes containing *tert*-amines and phosphines. The introduction of two electron-donating NMe_2 into the *ortho*-position of two P-linked phenyl rings in ligand **ppda**, two electron-withdrawing CF_3 into the *meta*-position of NMe_2 in ligand **pfda**, can sterically control the orientation of the ligands and vary photophysical property of the complexes. The emission color can change from blue to yellow. Complexes **1, 4** and **5** show delayed fluorescence, complexes **2**, **3** and **6** show prompt fluorescence, due to the difference in $\Delta E(S_1-T_1)$ values (small for the former, and large for the latter). And $\Delta E(S_1-T_1)$ values depend on the dihedral angles between CuX_2 plane and bridging N, P phenyl ring plane, two nearly orthogonal planes result in the large overlap between HOMO and LUMO and large $\Delta E(S_1-T_1)$ values. It is evident that the investigation of the relationship between structure and property helps us to understand the emitting process in guarding the further studies and application in OLEDs.

ACKNOWLEDGEMENTS

Li Liu thanks the financial support from the National Natural Science Foundation of China (21671061) and application foundation frontier special project from Wuhan Science and Technology Bureau (2019010701011414). Thanks to senior engineer Mingxing Chen (Peking University) for the photophysical measurements.

Supporting Information

The following files are available free of charge.

NMR and mass data, molecular structures, cyclic voltammogram, photophysical data, computational details, the device performance of doped device (PDF).

Accession Codes

CCDC 2051929−2051931 and 1897752-1897754 contain the supplementary crystallographic data for this paper. These data can be obtained free of charge via www.ccdc.cam.ac.uk/data_request/cif, or by emailing data_request@ccdc.cam.ac.uk, or by contacting The Cambridge Crystallographic Data Centre, 12 Union Road, Cambridge CB2 1EZ, UK; fax: +44 1223 336033.

AUTHOR INFORMATION

Corresponding Authors

Li Liu, Email: liulihubei@hubu.edu.cn,
Xin-Xin Zhong, Email: xxzhong@hubu.edu.cn
Lei Wang, E-mail: wanglei@mail.hust.edu.cn
Wai-Yeung Wong, E-mail: wai-yeung.wong@polyu.edu.hk

Author Contributions

Ke Xu, Bu-Lin Chen and Fei Yang contributed equally to this work. The manuscript was written through contributions of all authors. All authors have given approval to the final version of the manuscript.

Conflicts of interest Disclosure

There are no conflicts to declare.

ABBREIATIONS

OLED, organic light emitting diode; TADF, thermally activated delayed fluorescence; EQE, external quantum efficiency; HOMO, the highest occupied molecular orbital; LUMO, the lowest unoccupied molecular orbital; ITO, indium tin oxide; PEDOT, poly(3,4-ethylenedioxythiophene); PSS, poly(styrenesulfonate); TPBi, 1,3,5-Tris(1-phenyl-1H-benzimidazol-2-yl)benzene; CBP, 1,3-bis(9-carbazolyl)benzene.

REFERENCES

(1) Zhang, Q.; Komino, T.; Huang, S.; Matsunami, S.; Goushi, K.; Adachi, C. Triplet Exciton Confinement in Green Organic Light-Emitting Diodes Containing Luminescent Charge-Transfer Cu(I) Complexes. *Adv. Funct. Mater.* **2012**, *22*, 2327–2336.

(2) Tao, Y.; Yuan, K.; Chen, T.; Xu, P.; Li, H.; Chen, R.; Zheng, C.; Zhang, L.; Huang, W. Thermally Activated Delayed Fluorescence Materials Towards the Breakthrough of

Organoelectronics. *Adv. Mater*. **2014**, *26*, 7931-7958.

(3) Huitorel, B.; Moll, H. E.; Utrera-Melero, R.; Cordier, M.; Fargues, A., Garcia, A.; Massuyeau, F.; Martineau-Corcos, C.; Fayon, F.; Rakhmatullin, A.; Kahlal, S.; Saillard, J. Y.; Gacoin, T.; Perruchas, S. Evaluation of Ligands Effect on the Photophysical Properties of Copper Iodide Clusters. *Inorg. Chem.* **2018**, *57*, 4328-4339.

(4) Evariste, S.; Khalil, A. M.; Moussa, M. E.; Chan, A. K. W.; Hong, E. Y. H.; Wong, H. L.; Guennic, B. L.; Calvez, G.; Costuas, K.; Yam, V. W. W.; Lescop, C. Adaptive Coordination-driven Supramolecular Syntheses toward New Polymetallic Cu(I) Luminescent Assemblies. *J. Am. Chem. Soc.* **2018**, *140*, 12521-12526.

(5) Moussa, M. E. S.; Khalil, A. M.; Evariste, S.; Wong, H. L.; Delmas, V.; Guennic, B. L.; Calvez, G.; Costuas, K.; Yam, V. W. W.; Lescop, C. Intramolecular Rearrangements Guided by Adaptive Coordination-driven Reactions toward Highly Luminescent Polynuclear Cu(I) Assemblies. *Inorg. Chem. Front.* **2020**, *7*, 1334-1344.

(6) Hupp, B.; Nitsch, Jörn; Schmitt, T.; Bertermann, R.; Edkins, K.; Hirsch, F.; Fischer, I.; Auth, M.; Sperlich, A.; Steffen, A. Stimulus-triggered Anion-Cation-Exciplex Formation in Copper(I)-Complexes as new Mechanism for Mechanochromic Phosphorescence. *Angew. Chem. Int. Ed.* **2018**, *57*, 13671-13675.

(7) Hupp, B.; Schiller, C.; Lenczyk, C.; Stanoppi, M.; Edkins, K.; Lorbach, A.; Steffffen, A. Synthesis, Structures, and Photophysical Properties of a Series of Rare Near-IR Emitting Copper(I) Complexes. *Inorg. Chem.* **2017**, *56*, 8996-9008.

(8) Chakkaradhari, G.; Eskelinen, T.; Degbe, C.; Belyaev, A.; Melnikov, A. S.; Grachova, E. V.; Tunik, S. P.; Hirva, Pipsa; Koshevoy, I. O. Oligophosphine-thiocyanate Copper(I) and Silver(I) Complexes and Their Borane Derivatives Showing Delayed Fluorescence. *Inorg. Chem.* **2019**, *58*, 3646-3660.

(9) Chakkaradhari, G.; Chen, Y. T.; Karttunen, A. J.; Dau, M. T.; Janis, J.; Tunik, S. P.; Chou, P. T.; Ho, M. L.; Koshevoy, I. O. Luminescent Triphosphine Cyanide d^{10} Metal Complexes. *Inorg. Chem.* **2019**, *58*, 2174-2184.

(10) Czerwieniec, R.; Leitl, M. J.; Homeier, H. H. H.; Yersin, H. Cu(I) Complexes−Thermally Activated Delayed Fluorescence. Photophysical Approach and Material Design. *Coord. Chem. Rev.* **2016**, *325*, 2-28.

(11) Yersin, H.; Czerwieniec, R.; Shafikov, M. Z.; Suleymanova, A. F. TADF Material Design - Photophysical Background and Case Studies Focusing on Cu(I) and Ag(I) Complexes. *ChemPhysChem* **2017**, *18*, 3508-3535.

(12) Highly Efficient OLEDs-Materials Based on Thermally Activated Delayed Fluorescence, ed. Yersin, H., Germany, Wiley-VCH, Weinheim, 2019.

(13) Li, G.; Nobuyasu, R. S.; Zhang, B.; Geng, Y.; Yao, B.; Xie, Z.; Zhu, D.; Shan, G.; Che, W.; Yan, L.; Su, Z.; Dias, F. B.; Bryce, M. R. Thermally Activated Delayed Fluorescence in CuI Complexes Originating from Restricted Molecular Vibrations. *Chem. Eur. J.* **2017**, *23*, 11761-11766.

(14) Brown, C. M.; Li, C.; Carta, V.; Li, W.; Xu, Z.; Stroppa, P. H. F.; Samuel, I, D. W.; Zysman-Colman, E.; Wolf, M. O. Influence of Sulfur Oxidation State and Substituents on Sulfur-Bridged Luminescent Copper(I) Complexes Showing Thermally Activated Delayed Fluorescence. *Inorg. Chem.* **2019**, *58*, 7156−7168.

(15) Hashimoto, M.; Igawa, S.; Yashima, M.; Kawata, I.; Hoshino, M.; Osawa, M. Highly Efficient Green Organic Light-Emitting Diodes Containing Luminescent Three-Coordinate Copper(I) Complexes. *J. Am. Chem. Soc.* **2011**, *133*, 10348-10351.

(16) Hamze, R.; Peltier, J. L.; Sylvinson, D.; Jung, M.; Cardenas, J.; Haiges, R.; Soleihavoup, M.; Jazzar, R.; Djurovic, P. I.; Bertrand, G.; Thompson, M. E. Eliminating Nonradiative Decay in Cu(I) Emitters: >99% Quantum Efficiency and Microsecond Lifetime. *Science* **2019**, *363*, 601-606.

(17) Zhang, J.; Duan, C.; Han, C.; Yang, H.; Wei, Y.; Xu, H. Balanced Dual Emissions from Tridentate Phosphine-Coordinate Copper(I) Complexes toward Highly Efficient Yellow OLEDs. *Adv. Mater.* **2016**, *28*, 5975-5979.

(18) Volz, D.; Chen, Y.; Wallesch, M.; Liu, R.; Fléchon, C.; Zink, D. M.; Friedrichs, J.; Flügge, H.; Steininger, R.; Göttlicher, J.; Heske, C.; Weinhardt, L.; Bräse, S.; So, F.; Baumann, T. Bridging the Efficiency Gap: Fully Bridged Dinuclear Cu(I)-Complexes for Singlet Harvesting in High-Efficiency OLEDs. *Adv. Mater.* **2015**, *27*, 2538-2543.

(19) Leitl, M. J.; Küchle, F.; Mayer, H. A.; Wesemann, L.; Yersin, H. Brightly Blue and Green Emitting Cu(I) Dimers for Singlet Harvesting in OLEDs. *J. Phys. Chem. A* **2013**, *117*, 11823-11836.

(20) Tsuboyama, A.; Kuge, K.; Furugori, M.; Okada, S.; Hoshino, M.; K. Ueno. Photophysical Properties of Highly Luminescent Copper(I) Halide Complexes Chelated with 1,2-Bis(diphenylphosphino)benzene. *Inorg. Chem.* **2007**, *46*, 1992-2001.

(21) Verma, A.; Zink, D. M.; Fléchon, C.; Carballo, J. L.; Flügge, H.; Navarro, J. M.; Baumann, T.; Volz, D. Efficient, Inkjet-printed TADF-OLEDs with an Ultra-soluble NHetPHOS Complex. *Appl. Phys. A* **2016**, *122*, 191.

(22) Jia, J. H.; Chen, X. L.; Liao, J. Z.; Liang, D.; Yang, M. X.; Yu, R.; Lu, C. Z. Highly Luminescent Copper(I) Halide Complexes Chelated with a Tetradentate Ligand (PNNP): Synthesis, Structure, Photophysical Properties and Theoretical Studies. *Dalton Trans.* **2019**, *48*, 1418-1426.

(23) Zink, D. M.; Bächle, M.; Baumann, T.; Nieger, M.; Kühn, M.; Wang, C.; Klopper, W.; Monkowius, U.; Hofbeck, T.; Yersin, H.; Bräse, S. Synthesis, Structure, and Characterization of Dinuclear Copper(I) Halide Complexes with P^N Ligands Featuring Exciting Photoluminescence Properties. *Inorg. Chem.* **2013**, *52*, 2292-2305.

(24) Kang,;L.; Chen, J.; Teng, T.; Chen, X. L.; Yu, R.; Lu, C. Z. Experimental and Theoretical Studies of Highly Emissive Dinuclear Cu(I) Halide Complexes with Delayed Fluorescence. *Dalton Trans.* **2015**, *44*, 11649-11659.

(25) Li, X.; Zhang, J.; Zhao, Z.; Yu, X.; Li, P.; Yao, Y.; Liu, Z.; Jin, Q. H.; Bian, Z.; Lu, Z. Hong.; Huang, C. Bluish-green Cu(I) Dimers Chelated with Thiophene Ring-introduced Diphosphine Ligands for Both Singlet and Triplet Harvesting in OLEDs. *ACS Appl. Mater. Inter.* **2019**, *11*, 3262-3270.

(26) Li, X.; Zhang, J.; Wei, F.; Liu, X.; Liu, Z.; Bian Z., Huang, C. A Series of Dinuclear Cuprous Iodide Complexes Chelated with 1,2-Bis(diphenylphosphino)benzene Derivatives: Structural, Photophysical and Thermal Properties. *CrystEngComm*, **2016**, *18*, 4388-4394.

(27) Okano, Y.; Ohara, H.; Kobayashi, A.; Yoshida, M.; Kato, M. Systematic Introduction

of Aromatic Rings to Diphosphine Ligands for Emission Color Tuning of Dinuclear Copper(I) Iodide Complexes. *Inorg. Chem.* **2016**, *55*, 5227-5236.

(28) Gibbons, S. K.; Hughes, R. P.; Glueck, D. S.; Royappa, A. T.; Rheingold, A. L.; Arthur, R. B.; Nicholas, A. D.; Patterson, H. H. Synthesis, Structure, and Luminescence of Copper(I) Halide Complexes of Chiral Bis(phosphines). *Inorg. Chem.* **2017**, *56*, 12809-12820.

(29) Chen, B.; Liu, L.; Zhong, X. X.; Asiri, A. M.; Alamry, K. A.; Li, G. H.; Li, F. B.; Zhu, N. Y.; Wong, W. Y.; Qin, H. M. Synthesis, Characterization and Luminescent Properties of Copper(I) Halide Complexes Containing Biphenyl Bidentate Phosphine Ligand. *J. Coord. Chem.*, **2017**, *70*, 3907–3919.

(30) Wei, Q.; Chen, H. T.; Liu, L.; Zhong, X. X.; Wang, L.; Li, F. B.; Cong, H. J.; Wong, W. Y.; Alamrye, K. A.; Qin, H. M. Syntheses and Photoluminescence of Copper(I) Halide Complexes Containing Dimethylthiophene Bidentate Phosphine Ligands. *New J. Chem.* **2019**, *43*, 13408-13417.

(31) Hong, X.; Wang, B.; Liu, L.; Zhong, X. X.; Li, F. B.; Wang, L.; Wong, W. Y.; Qin, H. M.; Lo, Y. H. Highly Efficient Blue–green Neutral Dinuclear Copper(I) Halide Complexes Containing Bidentate Phosphine Ligands. *J. Lumin.* **2016**, *180*, 64-72.

(32) Wallesch, M.; Verma, A.; Fléchon, C.; Flügge, H.; Zink, D. M.; Seifermann, S. M.; Navarro, J. M.; Vitova, T.; Göttlicher, J.; Steininger, R.; Weinhardt, L.; Zimmer, M.; Gerhards, M.; Heske, C.; Bräse, S.; Baumann, T.; Volz, D. Towards Printed Organic Light-Emitting Devices: A Solution-Stable, Highly Soluble CuI–NHetPHOS Complex for Inkjet Processing. *Chem. Eur. J.* **2016**, *22*, 16400-16405.

(33) Volz, D.; Zink, D. M.; Bocksrocker, T.; Friedrichs, J.; Nieger, M.; Baumann, T.; Lemmer, U.; Bräse, S. Molecular Construction Kit for Tuning Solubility, Stability and Luminescence Properties: Heteroleptic MePyrPHOS-Copper Iodide-Complexes and their Application in Organic Light-Emitting Diodes. *Chem. Mater.* **2013**, *25*, 3414−3426.

(34) Araki, H.; Tsuge, K.; Sasaki, Y.; Ishizaka, S.; Kitamura, N. Luminescence Ranging from Red to Blue: A Series of Copper(I)-Halide Complexes Having Rhombic $\{Cu_2(\mu\text{-}X)_2\}$ (X = Br and I) Units with N-Heteroaromatic Ligands. *Inorg. Chem.* **2005**, *44*, 9667-9675.

(35) Araki, H.; Tsuge, K.; Sasaki, Y.; Ishizaka, S.; Kitamura, N. Synthesis, Structure, and Emissive Properties of Copper(I) Complexes $[Cu^{I}{}_2(\mu\text{-}X)_2(\mu\text{-}1,8\text{-naphthyridine})(PPh_3)_2]$ (X = I, Br) with a Butterfly-Shaped Dinuclear Core Having a Short Cu-Cu Distance. *Inorg. Chem.* **2007**, *46*, 10032-10034.

(36) Liang, P.; Kobayashi, A.; Sameera, W. M. C.; Yoshida, M.; Kato, M. Solvent-Free Thermal Synthesis of Luminescent Dinuclear Cu(I) Complexes with Triarylphosphines. *Inorg. Chem.* **2018**, *57*, 5929-5938.

(37) Kamtekar, K. T.; Monkman, A. P.; Bryce, M. R. Recent Advances in White Organic Light-Emitting Materials and Devices (WOLEDs). *Adv. Mater.* **2010**, *22*, 572–582.

(38) Zou, S. J.; Shen, Y.; Xie, F. M.; Chen, J. D.; Li, Y. Q.; Tang, J. X. Recent Advances in Organic Light-Emitting Diodes: Toward Smart Lighting and Displays. *Mater. Chem. Front.* **2020**, *4*, 788-820.

(39) Wei, Q.; Zhang, R.; Liu, L.; Zhong, X. X.; Wang, L.; Li, G. H.; Li, F. B.; Alamry, K. A.; Zhao, Y. From Deep Blue to Green Emitting and Ultralong Fluorescent Copper(I) Halide

Complexes Containing Dimethylthiophene Diphosphine and PPh_3 ligands. *Dalton Trans.* **2019**, *48*, 11448-11459.

(40) Guo, B. K.; Yang, F.; Wang, Y. Q.; Wei, Q.; Liu, L.; Zhong, X. X.; Wang, L.; Gong, J. K.; Li, F. B.; Wong, W. Y.; Alamry, K. A.; Zhao, Y. Efficient TADF-OLEDs with Ultra-soluble Copper(I) Halide Complexes Containing Non-symmetrically Substituted Bidentate Phosphine and PPh_3 ligands. *J. Lumin.* **2020**, *220*, 116963.

(41) Zhang, W. J.; Zhou, Z. X.; Liu, L.; Zhong, X. X.; Asiri, A. M.; Alamry, K. A.; Li, F. B.; Zhu, N. Y.; Wong, W. Y.; Qin, H. M. Highly-efficient Blue Neutral Mononuclear Copper(I) Halide Complexes Containing Bi- and Mono-dentate phosphine ligands. *J. Lumin.* **2018**, *196*, 425-430.

(42) Osawa, M.; Hoshino, M.; Hashimoto, M.; Kawata, I.; Igawa, S.; Yashima, M. Application of Three-coordinate Copper(I) Complexes with Halide Ligands in Organic Light-emitting Diodes that Exhibit Delayed Fluorescence. *Dalton Trans*. **2015**, *44*, 8369-8378.

(43) Wallesch, M.; Volz, D.; Zink, D. M.; Schepers, U.; Nieger, M.; Baumann, T.; Bräse, S. Bright Coppertunities: Multinuclear CuI Complexes with N–P Ligands and Their Applications. *Chem. Eur. J.* **2014**, *20*, 6578-6590.

(44) Penfold, T. J.; Karlsson, S.; Capano, G.; Lima, F. A.; Rittmann, J.; Reinhard, M.; Rittmann-Frank, M. H.; Braem, O.; Baranoff, E.; Abela, R.; Tavernelli, I.; Rothlisberger, U.; Milne, C. J.; Chergui, M. Solvent-Induced Luminescence Quenching: Static and Time-Resolved X-Ray Absorption Spectroscopy of a Copper(I) Phenanthroline Complex. *J. Phys. Chem. A* **2013**, *117*, 4591 –4601.

(45) Yersin, H.; Finkenzeller, W. J.; Walter, M. J.; Djurovich, P. I.; Thompson, M. E.; Tsuboyama, A.; Okada, S.; Ueno, K.; Chi, Y.; Chou, P.-T.; Yang, X.-H.; Jaiser, F.; Neher, D.; Xiang, H. F.; LAi, S. W.; Lai, P. T.; Che, C. M.; Tanaka, I.; Tokito, S.; Dijken, A. Van; Brunner, K.; Börner, H.; Langeveld, B. M. W.; Mak, C. S. K.; Nazeeruddin, M. K.; Klein, C.; Grätzel, M.; Zuppiroli, L.; Berner, D.; Bian, Z. Q.; Huang, C. H. Highly Efficient OLEDs with Phosphorescent Materials, 1st ed., Wiley-VCH, Weinheim, 2008.

(46) Bässler, H.; Köhler, A. Charge Transport in Organic Semiconductors. *Top. Curr. Chem.* **2012**, *312*, 1– 66.

(47) Uoyama, H.; Goushi, K.; Shizu, K.; Nomura, H.; Adachi, C. Highly Efficient Organic Light-emitting Diodes from Delayed Fluorescence. *Nature* **2012**, *492*, 234 –238.

Table of Contents

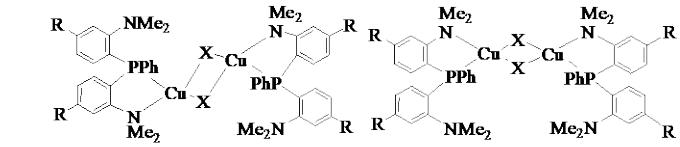

1: R = H, X = I
2: R = H, X = Br
3: R = H, X = Cl
4: R = CF_3, X = I
5: R = CF_3, X = Br

6: R = CF_3, X = Cl

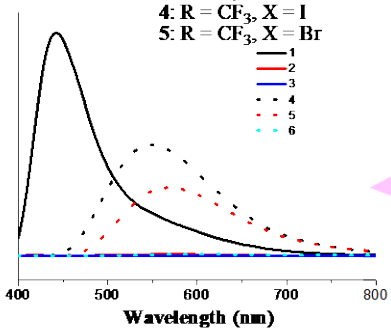

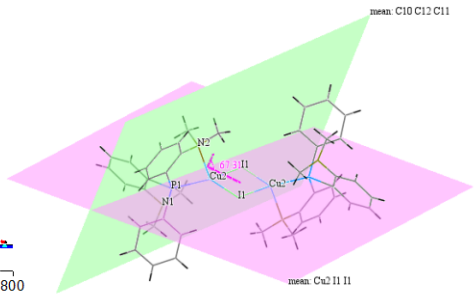

Complexes **1**, **4** and **5** exhibit intense blue to greenish yellow delayed fluorescence, complexes **2**, **3** and **6** show very weak yellowish green to yellow prompt fluorescence.